Regular Article

ANALYTICAL
AND BIOANALYTICAL
CHEMISTRY
RESEARCH

Published by the
Iranian Chemical Society

***Anal. Bioanal. Chem. Res.**, Vol. 2, No. 2, 73-84, December 2015.*

Removal of Dibenzothiophene Using Activated Carbon/γ-Fe_2O_3 Nano-Composite: Kinetic and Thermodynamic Investigation of the Removal Process

M. Fayazi[a,b,*], M.A. Taher[c], D. Afzali[d] and A. Mostafavi[c]

[a]*Mineral Industries Research Center, Shahid Bahonar University of Kerman, Kerman, Iran*

[b]*Young Researchers Society, Shahid Bahonar University, Kerman, Iran*

[c]*Department of Chemistry, Faculty of Sciences, Shahid Bahonar University, Kerman, Iran*

[d]*Department of Environment, Institute of Science and High Technology and Environmental Sciences, Graduate University of Advanced Technology, Kerman, Iran*

(Received 27 February 2015, Accepted 15 July 2015)

In the present study, removal of dibenzothiophene (DBT) from model oil (n-hexane) was investigated using magnetic activated carbon (MAC) nano-composite adsorbent. The synthesized nano-composite was characterized by FT-IR, FE-SEM, BET and VSM techniques. The MAC nano-composite exhibited a nearly superparamagnetic property with a saturation magnetization (M_s) of 29.2 emu g^{-1}, which made it desirable for separation under an external magnetic field. The magnetic adsorbent afforded a maximum adsorption capacity of 38.0 mg DBT g^{-1} at the optimized conditions (adsorbent dose, 8 g l^{-1}; contact time, 1 h; temperature, 25 °C). Langmuir, Freundlich and Temkin isotherm models were used to fit equilibrium data for MAC nano-composite. Adsorption process could be well described by the Langmuir model. Kinetic studies were carried out and showed the sorption kinetics of DBT was best described by a pseudo-second-order kinetic model. In addition, the MAC nano-composite exhibited good capability of recycling to adsorb DBT in gasoline deep desulfurization.

Keywords: Magnetic, Desulfurization, Activated carbon, Adsorbent, Dibenzothiophene

INTRODUCTION

Sulfur is a contaminant in fossil fuels and must be removed because it severely deactivates most catalysts including those used in automotive emissions control, petrochemicals production and fuel cells. The combustion of sulfur also produces precursors to acid rain; therefore its emission is regulated [1-6]. Clean fuels research has become an important subject of environmental catalysis studies, because more strict regulations on the level of contaminants are being implemented worldwide. The ultra-deep desulfurization of refinery streams is a key factor in obtaining ultra-low sulfur levels in fuels [7]. The removal of sulfur compounds from liquid fuels is carried out industrially by catalytic hydrodesulfurization (HDS). While conventional HDS has been highly effective for the reduction of sulfur levels, aromatic sulfur compounds such as thiophene, benzothiophene, dibenzothiophene (DBT) and their derivatives as the major objectionable sulfur components present in the petroleum fractions are less reactive to this process [8]. Dibenzothiophene is well-known representatives of the least reactive specie from this class [9-13]. However, catalytic HDS is not appropriate for further ultra-deep desulfurization because of the necessary use of more high-cost hydrogen and larger reactor volume, as well as undesirable changes in the fuel properties, such as color and octane number [14-17]. Meanwhile adsorptive desulfurization provides an alternative technology of particular interest due to its low-energy consumption, the availability of regeneration of spent adsorbent and the ambient operation temperature and pressure [18]. Hence, extensive efforts have been made to find adsorbent materials with both high capacity and good selectivity.

*Corresponding author. E-mail: maryam.fayazi@yahoo.com

Activated carbons (ACs) with well-developed porous structure and unique surface properties have exhibited good potential as adsorbents for sulfur compounds and their adsorption capacity can be further improved by modification [19]. An important step after adsorption of the desired compounds from the liquid sample is separation of the spent adsorbent from the medium, which is conventionally performed by filtration or centrifugation. As an alternative, a convenient method is to prepare magnetic adsorbents and attract them to an external magnetic field. Several studies have shown that incorporation of magnetic nano-particles (MNPs) into different types of carbons make this feasible [20-23]. MNPs with the general formula MFe_2O_4 (M = Fe, Co, Cu, Mn, *etc.*) such as magnetite (Fe_3O_4), maghemite (γ-Fe_2O_3), and cobalt oxide (Co_3O_4) are of the most popular materials in analytical biochemistry, medicine, removal of heavy metals, and biotechnology, and have been increasingly applied to immobilize proteins, enzymes, and other bioactive agents due to the advantages of easy control and simple separation [24-29]. It is believed that MNPs exhibit the finite-size effect or high ratio of surface-to-volume, resulting in a higher adsorption capacity. Maghemite nano-particles have attracted particular interest in separation science, because they can be easily isolated using an external magnetic field placed outside of the extraction container [30,31]. Furthermore, there are no diffusion limitations, since the available surface is totally external as the MNPs are nonporous. Combining the advantages of cheap activated carbon and magnetic nano-particles with an industrial friendly-production method may be a promising solution for the problem of the industrial production of the MAC nano-composite. Regarding the above comments, the aim of this research is production of MAC nano-composite without expensive organic solvent and complicated equipment and studied its performance for the first time for adsorption of DBT from model oils.

EXPERIMENTAL

Chemicals and Instruments

All reagents were of analytical grade. Ferric chloride ($FeCl_3$, 99%), ferrous chloride tetra hydrate ($FeCl_2.4H_2O$, 98%), ACs, hydrochloric acid (HCl, 37%), ammonium hydroxide (NH_4OH, 25-30%), dibenzothiophene (DBT, 98%), toluene (C_7H_8, 99.5%) and ethanol (C_2H_5OH, 99.9%) were purchased from Merck (Darmstadt, Germany). Double distilled deionized water was used throughout.

A Cary 50 single detector double beam in–time spectrophotometer (Varian, Australia) was used for determining the amount of analyte (DBT) retained by the adsorbent and recording the spectra as required. A water bath shaker model BM 402 (Nuve, Turkey) was used for mixing the solutions. The morphological evaluation was carried out by field emission scanning electron microscopy (FE-SEM, Hitachi S4160). Infrared (IR) spectra were recorded with KBr pellet on a Bruker tensor 27 Fourier transform infrared (FT-IR) spectrometer with RT-DLATGS detector, in the range of 400-4000 cm^{-1} with a spectral resolution of 4 cm^{-1} in transmittance mode. Magnetization measurement was performed using a vibration sample magnetometer (VSM) (Model PAR-VSM 155R). The specific surface area of AC and MAC nano-composite were characterized by the Brunaure-Emett-Teller (BET) method.

Preparation of Adsorbent

MAC nano-composite was synthesized as described by Darezereshki *et al*. [32]. As a pre-treating step, 20 g of purified activated carbon reacted with 150 ml 5 M nitric acid solution and refluxed for 1 h at 70 ºC to achieve treated activated carbon (TAC). The synthesis procedure for the nano-composite was as follows: 4.2 g of TAC, 13 g of $FeCl_3$ (99%) and 8 g of $FeCl_2.4H_2O$ (98%) were dissolved in 100 ml of 2 M HCl (37%). Then, NH_4OH (25-30%) solution (2 M) was added dropwise into this solution (300 ml) under vigorous stirring at room temperature for 2 h. The obtained dark brown precipitate was separated from the reaction medium by magnetic field. After seven times of rinsing the precipitate under deionized water and absolute ethanol (99.93%), it was dried at 70 ºC overnight. The synthesized MAC nano-composite exhibited a nearly super paramagnetic property with a saturation magnetization (M_s) of 29.2 emu g^{-1}A, which made it desirable for separation under an external magnetic field.

DBT Adsorption Studies Using Magnetic Active Carbon

A solution 600 mg Kg^{-1} DBT in n-hexane was used for adsorption studies. In each experiment, approximately 0.08

g of MAC nano-composite was mixed with 10 ml of the DBT solution and shaked at 200 rpm under atmospheric pressure at 25 °C for 40 min. Then, the MAC nano-composite was separated by a magnet. The residual DBT in solution was measured by UV-Vis spectrophotometry at 326 nm. The amount of DBT adsorbed (q_e) by the adsorbent was calculated using the equation:

$$q_e = \frac{[(C]_0 - C_e)w}{m} \quad (1)$$

where q_e (mg g^{-1}) is the equilibrium amount adsorbed, w (Kg) is the amount of the liquid phase, C_0 (mg Kg^{-1}) is the initial concentration of DBT before exposed to absorbent, C_e (mg Kg^{-1}) is the concentration of DBT at equilibrium, and m (g) is the mass of the absorbent. The amount of DBT adsorbed onto the MAC nano-composite at any time (q_t) was obtained from the following relationship:

$$q_t = \frac{[(C]_0 - C_t)w}{m} \quad (2)$$

where C_t is the bulk concentration (mg Kg^{-1}) of DBT at any time t.

RESULTS AND DISCUSSION

Nano-Composite Characterization

FT-IR spectra of AC, γ-Fe_2O_3 and MAC nano-composites are shown in Fig. 1. Absorption peaks appearing at 453, 581, 630, 797 and 889 cm^{-1} in the FT-IR spectra are attributed to γ-Fe_2O_3 nano-particles existing in the activated carbon. The phenomena could be related to the formation of maghemite nano-particles inside the pores. Figure 2 presents the morphology image of TAC and MAC nano-composite obtained from the FE-SEM analysis. As can be seen from Fig. 2b, the maghemite nano-particles deposited on the surface of activated carbon are uniform with the spherical shape. The magnetic hysteresis loops of AC and MAC are illustrated in Fig. 3. The saturation magnetisation of the magnetic nano-composite was measured as 29.2 emu g^{-1}. This magnetic susceptibility value is sufficient for this adsorbent to be used in wastewater treatment, which can be used for the magnetic separation (inset in Fig. 3). The specific surface areas of TAC and MAC nano-composite were measured from the N_2 adsorption/desorption isotherms using the BET method. According to BET theory, the specific surface area was calculated as 598 m^2 g^{-1} for TAC and 367 m^2 g^{-1} for MAC.

Effect of Temperature on Adsorption

The effect of temperature on the adsorption of DBT on MAC nano-composite was investigated by adding 0.08 g of the magnetic adsorbent into 10 ml of 600 mg Kg^{-1} DBT and shaking the mixture for 120 min at different temperatures of 10-60 °C in a water bath. The results show that the equilibrium adsorption amount increases slowly with increasing temperature (Fig. 4), indicating that the adsorption process is endothermic. The increase in the amount of DBT adsorbed on the MAC nano-composite with temperature can be attributed to an increased mobility of the DBT molecules in solution and within the sorbent porous structure overcoming the activation energy barrier. These results illustrate that the temperature is less important for the desulfurization performance.

Effect of Mass of Adsorbents

The effect of adsorbent dosage (m) on the amount of DBT adsorbed also investigated. The amounts of DBT adsorbed on to MAC are shown in Fig. 5. The results indicated that the amount of DBT adsorbed increased as the MAC nano-composite dosage increased and then remains almost unchanged when 80 mg of MAC nano-composite was used. After that, even though the adsorbent dosage increases in the adsorption system, because of the unavailability of the adsorbate, the percentage adsorption remains constant. Therefore, absorbent dosage 80 mg was chosen in further experiments.

Effect of Shaking Time

To find the equilibrium shaking time for the adsorption of DBT on MAC adsorbent, the adsorption study was carried out at different time intervals ranging from 5-180 min, while other experimental conditions such as: initial DBT concentration (600 mg Kg^{-1}), volume of solution (10 ml), adsorbent dose (80 mg) and temperature (25 °C) were kept constant, and the results are shown in Fig. 6. It seems that the adsorption process has a two-stage kinetic behavior; rapid initial adsorption followed by a second stage with a

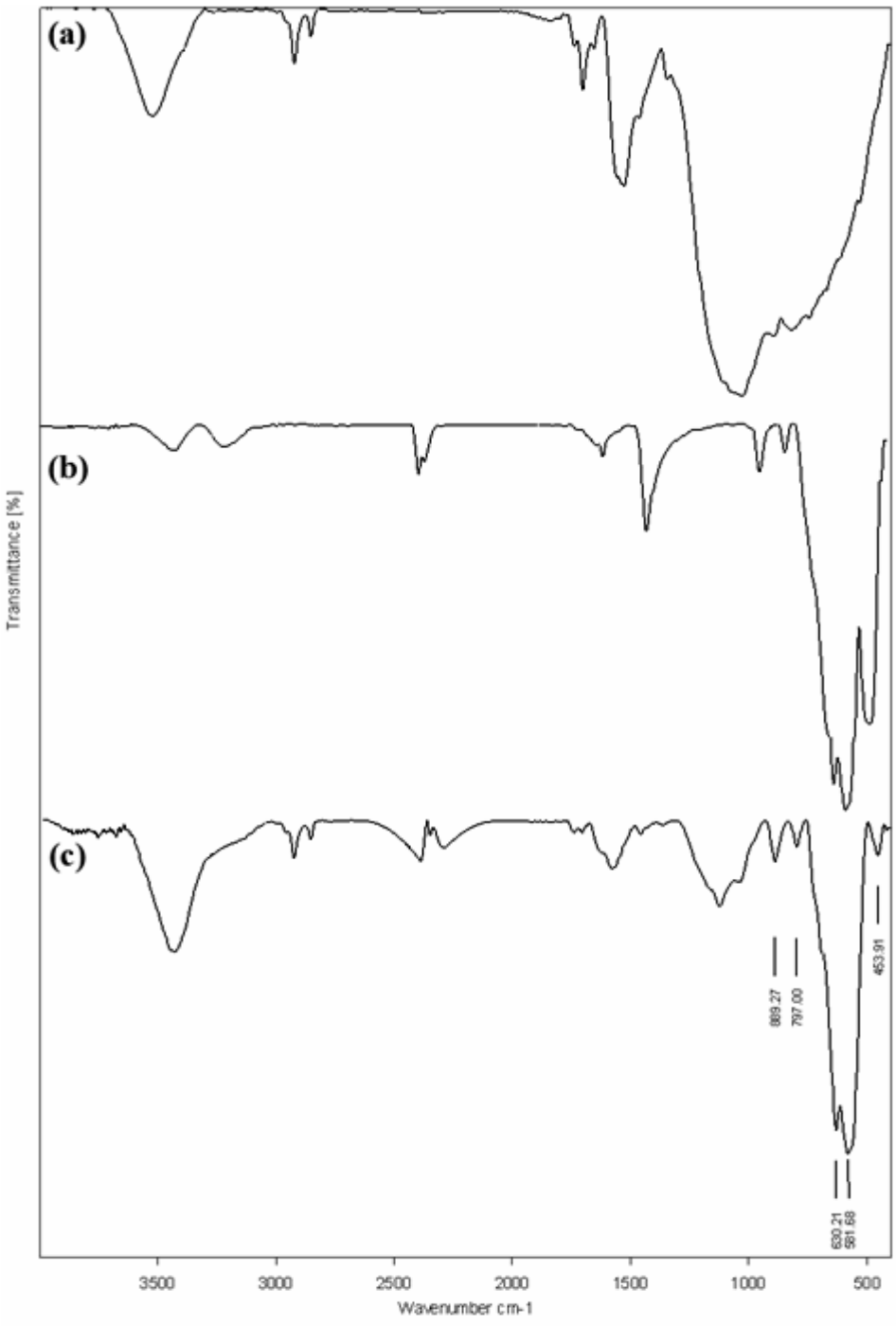

Fig. 1. FT-IR spectra of (a) TAC, (b) maghemite and (b) MAC nano-composite.

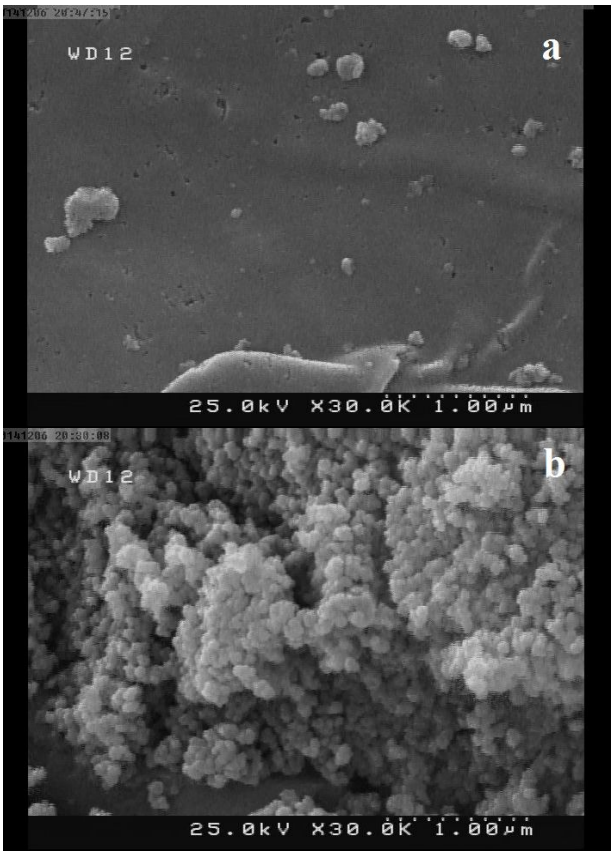

Fig. 2. (a) FE-SEM images of TAC and (b) MAC nano-composite.

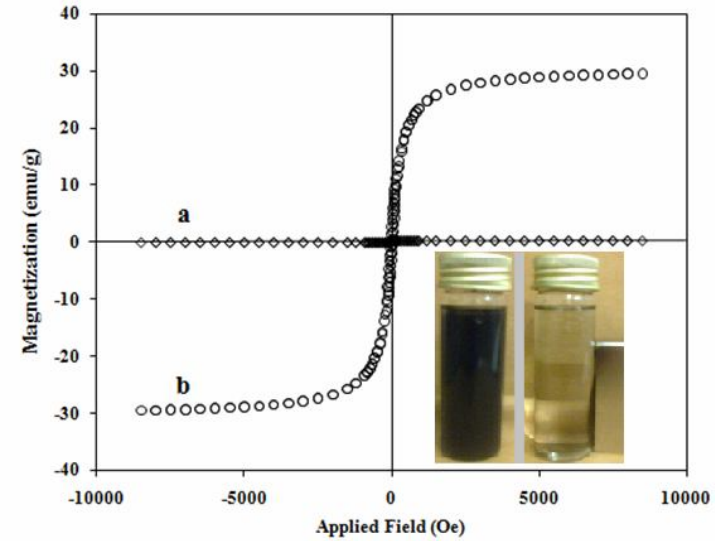

Fig. 3. Magnetic hysteresis curves of (a) AC, (b) MAC nano-composite. The bottom inset shows the magnetic separation of the MAC under an external magnetic field.

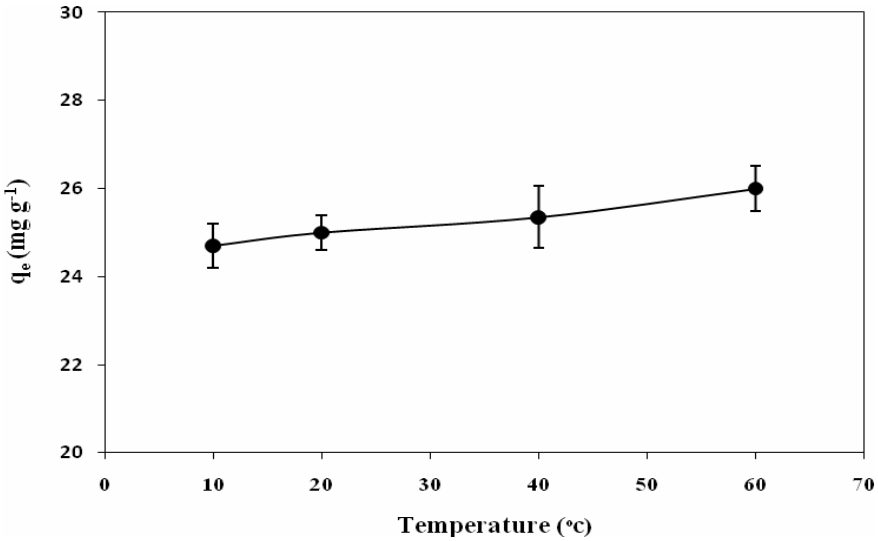

Fig. 4. Effect of temperature in the range of 10-60 °C on the adsorption of DBT by MAC.

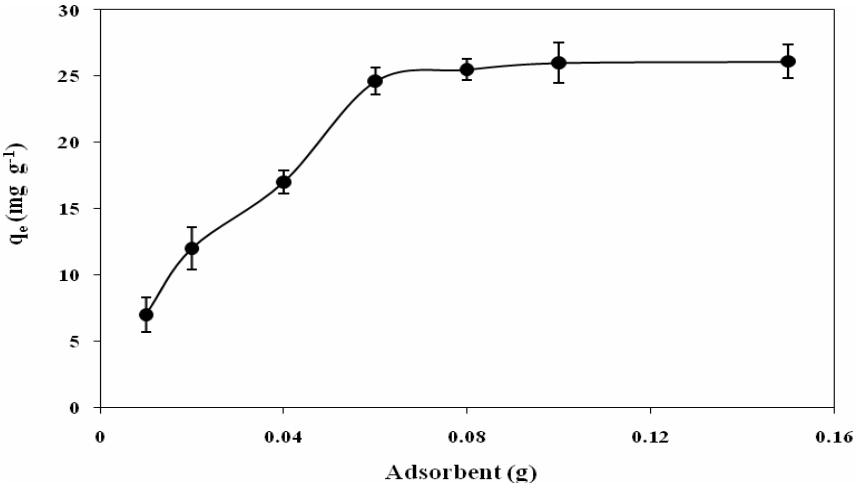

Fig. 5. Effect of the amount of adsorbent on DBT adsorption capacity of MAC at 25 °C.

much lower adsorption rate. The results indicate that most of the DBT is removed within 20 min at which the adsorption amount (q_t) is ~38 mg g^{-1}, and almost levels off after this period, so that the DBT uptake remains almost unchanged with increasing the contact time, indicating that all adsorption sites have been saturated. We used 40 min of continuous shaking, at which a steady state approximation can be assumed and a quasi-equilibrium situation can be accepted.

Effect of Initial DBT Concentration

To examine the effect of initial DBT concentration, different concentration in the range of 100-1100 mg Kg^{-1} onto 8 g l^{-1} MAC at 25 °C using contact time of 40 min were investigated, that results is shown in Fig. 7. As can be seen, the adsorption of DBT per unit mass of the adsorbent increases with increasing initial DBT concentration. The equilibrium adsorption of DBT increased from 12.1-30.5 mg g^{-1} adsorbent when the initial concentration of DBT

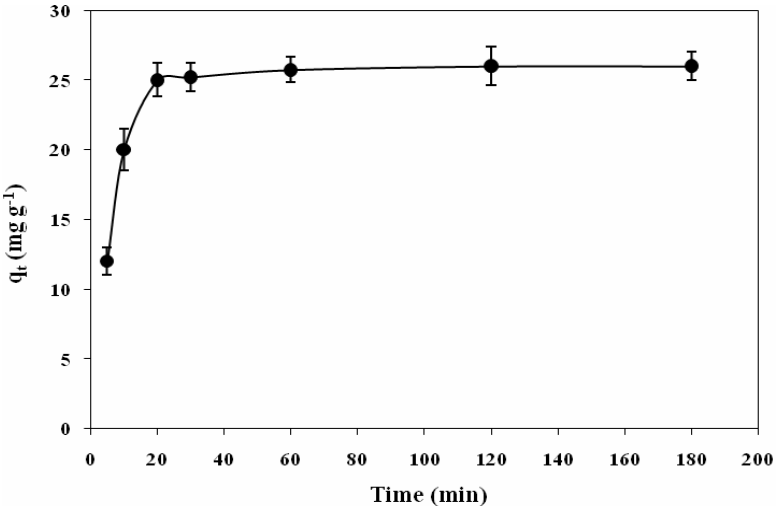

Fig. 6. Effect of the shaking time on DBT adsorption capacity onto MAC at 25 °C.

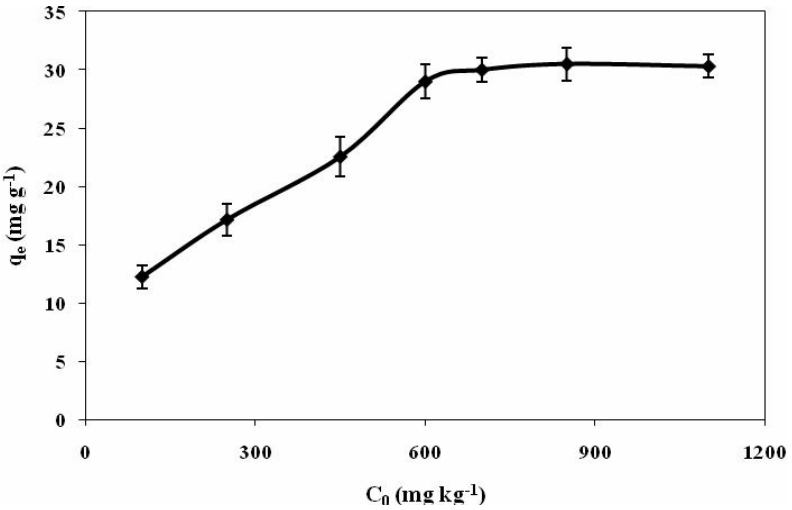

Fig. 7. Effect of initial concentration of DBT on adsorption.

increased from 100-1100 mg kg^{-1}. The increase of DBT adsorption with respect to its initial concentration is a result of the increase in mass transfer driving force due to concentration gradient developed between the bulk solution and surface of the adsorbent [33].

Adsorption Kinetics

The kinetic data obtained were analyzed using pseudo-first-order rate Eq. (3) and pseudo-second-order rate Eq. (4), respectively.

$$ln(q_e - q_t) = lnq_e - k_1 t \quad (3)$$

$$\frac{t}{q_t} = \frac{1}{k_2 q_e^2} + \left(\frac{1}{q_e}\right)t \quad (4)$$

where q_e and q_t (mg g^{-1}) are the amount of DBT molecular

Table 1. Pseudo-First-Order and Pseudo-Second-Order Kinetic Model for Adsorption of DBT on MAC Nano-Composite

Initial DBT concentration (mg kg^{-1})	Pseudo-first-order model		Pseudo-second-order model			
	k_1 (min^{-1})	R^2	Exp. q_e (mg g^{-1})	Cal. q_e (mg g^{-1})	k_2 (g mg^{-1} min^{-1})	R^2
600	0.0674	0.8266	26	26.5	0.0135	0.9994

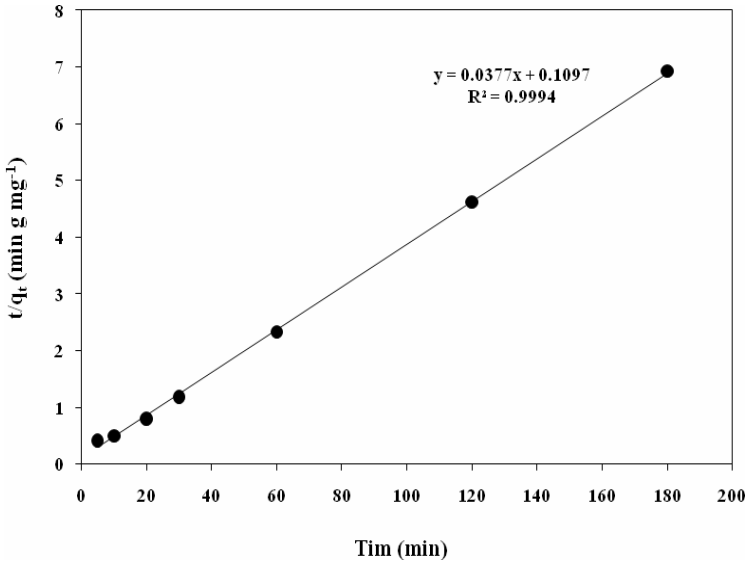

Fig. 8. DBT adsorption on to MAC using pseudo-second-order kinetics.

adsorbed on the sorbent at the equilibrium and at time *t* (min), respectively. k_1 (min^{-1}) and k_2 (g mg^{-1} min^{-1}) are the rate constant of adsorption. All the rate constants of adsorption and linear regression correlation coefficients were presented in Table 1. As illustrated in Table 1, the second-order model was more suitable to describe the sorption kinetic data than the first-order model because of the favorable fit between experimental and calculated values of q_e in the second-order model (R^2 values above 0.999). The plot of t/q_t *vs.* *t* based on pseudo-second-order kinetics are compiled in Fig. 8.

Adsorption Isotherms

The distribution of DBT molecules between the liquid and solid phases at equilibrium can be expressed by adsorption isotherms. The Langmuir, Freundlich and Temkin isotherms are widely used to describe the adsorption phenomena at the solid–liquid interface. The Langmuir relation assumes monolayer sorption on to the homogeneous surface with a specific number of equivalent sites.

The equilibrium expression of the Langmuir model is:

$$q_e = \frac{q_{max} \square (K_L C_e)}{1 + K_L C_e} \quad (5)$$

where q_{max} is the theoretical maximum adsorption capacity at monolayer (mg g^{-1}), and K_L is the Langmuir constant (Kg mg^{-1}).

The characteristic constants of the Langmuir model

can be determined from the linearized form of Eq. (6):

$$\frac{C_e}{q_e} = \frac{1}{q_{max} K_L} + \frac{C_e}{q_{max}} \quad (6)$$

Thus, plots of q_e *vs.* C_e should show a linear relationship, which is true in the case of this data as Fig. 9a, and so allows the determination of the q_{max} and k_L values, from the slope and intercept of the linear plot, respectively.

The Freundlich relation describes multilayer sorption and can be expressed as:

$$lnq_e = lnK_F + \frac{1}{n} lnC_e \quad (7)$$

where K_F and n are Freundlich constants demonstrating adsorption capacity and intensity, respectively.

Figure 9b shows the Freundlich plot (lnq_e *vs.* lnC_e) for the adsorption data, and the fitted results.

The Temkin isotherm was also applied to the adsorption of DBT on MAC. This model is given by the following linearized form:

$$q_e = B_T lnK_T + B_T lnC_e \quad (8)$$

where B_T and K_T are the Temkin constants. Figure 9c shows the Temkin plot (q_e *vs. lnCe*) for the adsorption data, and the fitted results.

As shown in Table 2, the linear regression analysis by the Langmuir, Freundlich and Temkin isotherms show a correlation coefficient (R^2) of 0.9964, 0.9717 and 0.9942, respectively. Accordingly, the adsorption of DBT on MAC nano-composite follows Langmuir isotherm model.

Adsorption Thermodynamics

The thermodynamic characteristics of the adsorption process could be reflected in these parameters: the standard free energy change (ΔG^o), the standard enthalpy change (ΔH^o), and the standard entropy change (ΔS^o). The thermodynamic parameters were calculated using the following Eqs. (9, 10):

$$\Delta G^o = -RT\, lnK_L \quad (9)$$

$$\Delta G^o = \Delta H^o - T\Delta S^o \quad (10)$$

The value of ΔG° was calculated to be -29.5 KJ mol^{-1}. The negative value of ΔG^o was confirmed that adsorption occurs spontaneously. Whereas equilibrium adsorption amount increases slowly with increasing temperature, therefore, value of ΔH^o is positive; therefore, value of ΔS^o is positive, this confirming a high preference of DBT molecules for the adsorbent surface.

Regeneration of the Adsorbent

For the industrial applications, the regeneration and subsequent recycling of the adsorbent are of vital importance. To test the reusability of absorbents, 0.08 g spent absorbents which was saturated after desulfurization of 10 ml DBT was washed with toluene. Spent adsorbent adding to 10 ml of extracting solvent (toluene) and the mixture was shaken at room temperature for 1 h. The washed absorbent was dried at 120 ºC overnight to remove the remaining toluene. Then the recycled absorbent was reused in desulfurization of 10 ml DBT again. By this solvent-washing method, the absorbents were reused for three times. The regeneration afforded 96, 92 and 78% of the initial adsorption capacity after the first three regeneration cycles, respectively. Low recycle number of proposed adsorbent may have been caused by the incomplete removal of DBT during washing.

Comparison with other Methods

A comparison was carried out between the results of the performance of proposed sorbent with those reported in previous studies. As can be seen from Table 3, the sorption capacity of MAC nano-composite is higher than those of activated carbon loaded with cerium [19], hollow molecular imprinted polymer [34], mesoporous carbon-silica nano-composite *via* copper modification [35], cerium/nickel-exchanged zeolite Y [36], carbon aerogels [37] but lower than that of nanoporous carbon [33] and magnetic mesoporous carbon [38]. Additionally, the inherent magnetic property of MAC nano-composite make it more efficient sorbent for the removal of DBT from aqueous solution. On the other hand, time of DBT adsorption with proposed magnetic composite is lower than of other methods.

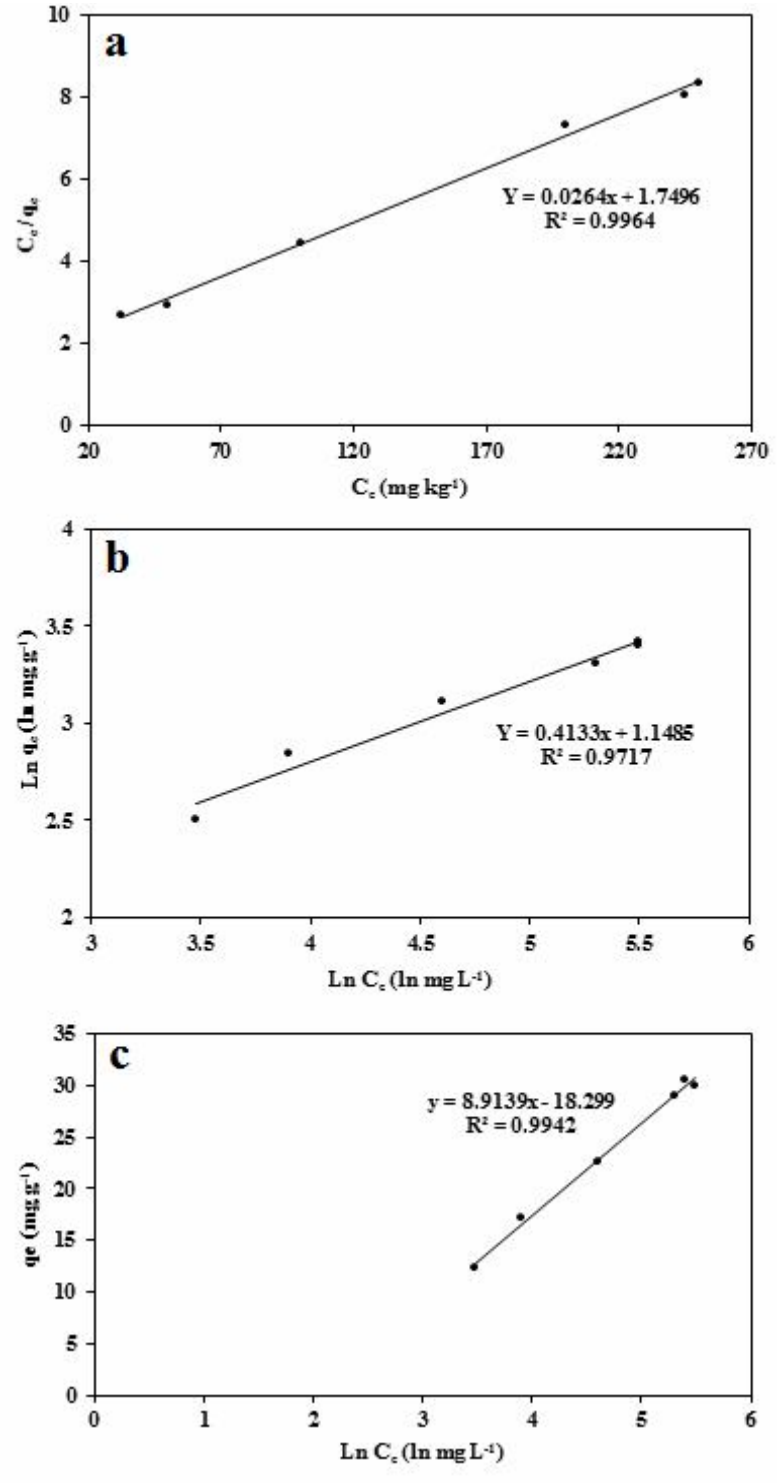

Fig. 9. Experimental adsorption data fitted to (a) Langmuir, (b) Freundlich and (c) Temkin models.

Table 2. Summary of Parameters Calculated from Fitting the Results of Adsorption Isotherm of DBT on MAC Nano-Composite to Different Models

Langmuir			Freundlich			Temkin		
q_{max} (mg g^{-1})	K_L (kg mg^{-1})	R^2	K_F (mg g^{-1}) (kg $mg^{-1})^{1/n}$	n	R^2	K_T (kg mg^{-1})	B_T (J mol^{-1})	R^2
38.0	0.0150	0.9964	3.15	2.42	0.9717	0.128	8.914	0.9942

Table 3. Comparison of Various Adsorbents for DBT Removal

Adsorbents	Adsorption capacity (mg g^{-1})	Adsorbent dosage (g)	Concentration (mg l^{-1})	Adsorption time (min)	Ref.
Activated carbon loaded with cerium	10.2	0.75	500	1080	[19]
Nanoporous carbon	294	0.02	1000	360	[33]
Hollow molecular imprinted polymer	31.55	0.01	100	180	[34]
Mesoporous carbon-silica nano-composite *via* copper modification	13.954	0.1	320	2880	[35]
Cerium/nickel-exchanged zeolite Y	22.2	0.1	500	180	[36]
Carbon aerogels	15.1	0.16	250	96	[37]
Magnetic mesoporous carbon	62.0	0.05	654.8	60	[38]
Activated carbon/γ-Fe_2O_3 nano-composite	38	0.08	393	40	This work

CONCLUSIONS

In this study, MAC nano-composite was successfully synthesized by a single-step wet chemical method at room temperature without using organic solvents and expensive raw materials. The prepared MAC nano-composite exhibited excellent specific recognition and saturation magnetization. The MAC nano-composite was used for adsorption of the aromatic sulfur compound (DBT). It could be easily separated from the suspension by an external magnetic field, which enables an easy separation process. For DBT adsorbed onto MAC nano-composite, the pseudo-second-order model yielded a better fit than those by the pseudo-first-order model and the equilibrium data were best described by the Langmuir isotherm model. The value of ΔG^0 was calculated to be -29.5 KJ mol^{-1}, indicating that the DBT adsorption by MAC nano-composite is a spontaneous and favorable process. The results obtained show that MAC nano-composite can be used for separation of DBT from liquid samples, and it could potentially substitute other more expensive adsorbents. Its advantages include ease of preparation, relatively low cost, and good adsorption properties. Also, adsorbent provides an easy separation process because it can be separated from the medium using a magnet. The spent adsorbent can be reused after regeneration by solvent extraction with toluene.

REFERENCES

[1] D.D. Beck, J.W. Sommers, C.L. DiMaggio, Appl. Catal. B 3 (1994) 205.

[2] A. Shamsi, Catal. Today 139 (2009) 268.

[3] J.J. Strohm, J. Zheng, C. Song, J. Catal. 238 (2006) 309.

[4] B.D. Gould, O.A. Baturina, K.E. Swider-Lyons, J. Power Sources 188 (2009) 89.

[5] L.J. Hoyos, H. Praliaud, M. Primet, Appl. Catal. A 98 (1993) 125.

[6] T. Wang, A. Vazquez, A. Kato, L.D. Schmidt, J. Catal. 78 (1982) 306.

[7] P. Torres-Mancera, J. Ramírez, R. Cuevas, A. Gutiérrez-Alejandre, F. Murrieta, R. Luna, Catal. Today 107 (2005) 551.

[8] C. Song, Catal. Today 86 (2003) 211.

[9] J.N. Díaz de León, M. Picquart, L. Massin, M. Vrinat, J.A. de los Reyes, J. Mol. Catal. A: Chem. 363 (2012) 311.

[10] X. Li, J. Bai, A. Wang, R. Prins, Y. Wang, Top. Catal. 54 (2011) 290.

[11] H. Wang, R. Prins, J. Catal. 264 (2009) 31.

[12] M. Houalla, D.H. Broderick, A.V. Sapre, N.K. Nag, V.H.J. de Beer, B.C. Gates, H. Kwart, J. Catal. 61 (1980) 523.

[13] H. Farag, K. Sakanishi, I. Mochida, D.D. Whitehurst, Energ. Fuel. 13 (1998) 449.

[14] S. Kumagai, H. Ishizawa, Y. Toida, Fuel 89 (2010) 365.

[15] I. Mochida, K. Sakanishi, X. Ma, S. Nagao, T. Isoda, Catal. Today 29 (1996) 185.

[16] F. van Looij, P. van der Laan, W.H.J. Stork, D.J. DiCamillo, J. Swain, Appl. Catal. A 170 (1998) 1.

[17] Y. Yoshimura, M. Toba, H. Farag, K. Sakanishi, Catal. Surv. Asia 8 (2004) 47.

[18] R.T. Yang, A.J. Hernández-Maldonado, F.H. Yang, Science 301 (2003) 79.

[19] L. Xiong, F.-X. Chen, X.-M. Yan, P. Mei, J. Porous Mat. 19 (2012) 713.

[20] Z.M. Sheng, J.N. Wang, Carbon 47 (2009) 3271.

[21] M. Baikousi, A.B. Bourlinos, A. Douvalis, T. Bakas, D.F. Anagnostopoulos, J. Tuček, K. Šafářová, R. Zboril, M.A. Karakassides, Langmuir 28 (2012) 3918.

[22] Z. Liu, Y. Song, Y. Yang, J. Mi, L. Deng, Mater. Res. Bull. 47 (2012) 274.

[23] Y. Zhai, Y. Dou, X. Liu, S.S. Park, C.-S. Ha, D. Zhao, Carbon 49 (2011) 545.

[24] A. Kraus, K. Jainae, F. Unob, N. Sukpirom, J. Colloid Interf. Sci. 338 (2009) 359.

[25] A.-H. Lu, E.L. Salabas, F. Schüth, Angew. Chem. Int. Ed. 46 (2007) 1222.

[26] A. Afkhami, R. Norooz-Asl, Colloid Surface A 346 (2009) 52.

[27] A. Afkhami, R. Moosavi, J. Hazard. Mater. 174 (2010) 398.

[28] A. Afkhami, R. Moosavi, T. Madrakian, Talanta 82 (2010) 785.

[29] A. Afkhami, M. Saber-Tehrani, H. Bagheri, Desalination 263 (2010) 240.

[30] A. Ahmadi, S. Heidarzadeh, A.R. Mokhtari, E. Darezereshki, H.A. Harouni, J. Geochem. Explor. 147 (2014) 151.

[31] E. Darezereshki, F. Tavakoli, F. Bakhtiari, A.B. Vakylabad, M. Ranjbar, Mater. Sci. Semicond. Process. 27 (2014) 56.

[32] E. Darezereshki, F. Bakhtiari, A.B. Vakylabad, Z. Hassani, Mater. Sci. Semicond. Process. 16 (2013) 221.

[33] M. Anbia, Z. Parvin, Chem. Eng. Res. Des. 89 (2011) 641.

[34] W. Yang, L. Liu, W. Zhou, W. Xu, Z. Zhou, W. Huang, Appl. Surf. Sci. 258 (2012) 6583.

[35] J. Cheng, S. Jin, R. Zhang, X. Shao, M. Jin, Micropor. Mesopor. Mat. 212 (2015) 137.

[36] J. Wang, F. Xu, W.-J. Xie, Z.-J. Mei, Q.-Z. Zhang, J. Cai, W.-M. Cai, J. Hazard. Mater. 163 (2009) 538.

[37] S. Haji, C. Erkey, Ind. Eng. Chem. Res. 42 (2003) 6933.

[38] N. Farzin Nejad, E. Shams, M.K. Amini, J.C. Bennett, Fuel Process. Technol. 106 (2013) 376.